ALPHA STORAGE REGIME IN HIGH TEMPERATURE SUB-IGNITED D-T TOKAMAKS

S.J. ZWEBEN, H.P. FURTH, D.R. MIKKELSEN, M.H. REDI, J.D. STRACHAN (Princeton Plasma Physics Laboratory, Princeton University, Princeton, New Jersey, United States of America)

ABSTRACT. Alpha particle parameters in sub-ignited D–T tokamaks such as TFTR can be optimized in a high temperature 'alpha storage regime' in which the alpha particle thermalization time τ_α is long ($\approx$1.0 s) and in which the alpha particle source rate S_α is enhanced because of beam–target and beam–beam reactions (by a factor of $\approx$2–4). Near reactor-level alpha instability parameters, $\beta_\alpha(0) \approx n_\alpha(0)/n_e(0) \approx 1\%$, are predicted by simulation codes when $Q \gtrsim 0.5$; present TFTR 'supershots' already have $\beta_\alpha(0) \approx n_\alpha(0)/n_e(0) \approx 0.1$–$0.2\%$. This alpha storage regime can be used for the first time to test theories of collective alpha instabilities and can also be used to provide a strong (but transient) alpha heating pulse. An experimental scenario to exploit this regime is described.

1. INTRODUCTION

This letter describes how sub-ignited D–T fuelled tokamaks such as TFTR or JET can be used to study reactor relevant alpha particle physics. This physics is important for future ignited plasmas since it could affect the alpha heating efficiency, the plasma confinement or the plasma beta limits.

Most of these new effects concern the influence of a high energy alpha particle component on plasma instabilities and so involve dimensionless parameters such as n_α/n_e (the alpha particle density over the electron density) and β_α (the ratio of perpendicular alpha energy to magnetic field energy), where both these parameters refer only to alpha particles with energies above $3kT_i/2$. These parameters depend on the product of the alpha source rate S_α and the alpha thermalization time τ_α; thus they are only indirectly related to the thermal plasma confinement time and energy balance parameters such as Q (fusion power multiplication factor) or the ignition margin.

Since $S_\alpha \propto P_{heat}\, Q$ and $\tau_\alpha \propto T_e/n_e$ (see Section 3.1), the local alpha density scales roughly as $n_\alpha \propto P_{heat}\, Q\, T_e/n_e$. Thus the alpha instability parameters tend to be maximized in high temperature, low density plasmas such as the TFTR 'supershots' [1], in which both S_α and τ_α tend to be high. Therefore, if the alpha particles are confined classically, τ_α can be very long ($\tau_\alpha \approx 1\ s \gg \tau_E$), allowing reactor level alpha parameters to be obtained even in sub-ignited $Q \approx 1$ machines such as TFTR and JET.

The other main aspect of reactor relevant alpha physics concerns the effect of alpha heating on the plasma. Although the alpha heating averaged over space and time is only $\langle P_\alpha/P_{heat}\rangle \approx 0.2$ at $Q \approx 1$, we show here how plasmas with $\langle P_\alpha/P_{heat}\rangle \approx 0.5$ and $P_\alpha(0)/P_{heat}(0) \approx 0.8$ can be transiently produced by thermalizing the stored alphas after auxiliary heating is turned off.

We call this high τ_α mode of operation the 'alpha storage regime'; this terms is intended to include the alpha 'storing' phase during auxiliary heating, the alpha 'coasting' phase just after auxiliary heating and the transient alpha 'heating' phase. The 'storage' aspect refers to the expected very long confinement time of alphas (somewhat analogous to a high energy particle storage ring).

This letter describes various estimates and simulations for this regime, with particular application to TFTR. Section 2 gives a brief summary of the alpha physics issues. Section 3 presents simplified analytic estimates of expected alpha parameters. More self-consistent code calculations for TFTR are given in Section 4. The present capabilities of TFTR with respect to these parameters are described in Section 5, and the conclusions are given in Section 6.

2. ALPHA PHYSICS ISSUES

A summary of the alpha instabilities and their possible effects is given in Table I, which is adapted from recent reviews [2]. For the purpose of this table, the instabilities are ordered in terms of their frequency, which ranges from $\approx 10^1$ to 10^9 Hz for TFTR.

Note that the instabilities in Table I are all 'collective' alpha effects, which means that the free energy of the D–T generated high energy alpha particle population either creates or modifies these instabilities. In addition to these D–T collective effects, alpha particles can also be influenced as 'single particles' by toroidal field ripple or by plasma instabilities that are not modified by alphas. However, single-particle physics is not discussed here since experiments on these effects can be done with D–D or D–^{3}He discharges [3].

At present, it is not easy to assess the eventual importance of these instabilities for ignited plasmas, partly because the theories are incomplete, but mostly because experimental conditions under which these

TABLE I. COLLECTIVE ALPHA INSTABILITIES*

Instability	TFTR frequency	Physical mechanism(s)	Important parameters	Possible effects
Alpha driven sawteeth	≥10 Hz	Central electron heating by alphas → sawtooth crash	$\frac{P_\alpha(0)}{P_{heat}(0)}$	Modification of q(r) profile; expulsion of alphas from centre
Alpha driven fishbones	$\gtrsim 10^4$ Hz	Resonance of alpha precession and internal m = 1 mode	$\beta_\alpha(0)$, $\beta_{th}(0)$, $\omega_{d\alpha}/\omega_A$	Expulsion of trapped alphas (1/4–1/3 of all alphas)
Alpha driven drift wave or ballooning modes	$\gtrsim 10^5$ Hz	Resonance with $m \gg 1$ modes	n_α/n_e, β_α, β_{th} and gradients	Effect on beta limits; effects on plasma transport coefficients
Alpha driven Alfvén waves	10^5–10^7 Hz ($\omega \ll \omega_{c\alpha}$)	$v_\alpha \cong v_A$ excites Alfvén modes	V_α/V_A, $\omega_{*\alpha}/\omega_A$, $\nabla\beta_\alpha$	Anomalous alpha transport; electron heating
Alpha loss cone driven Alfvén waves	$\sim 10^8$ Hz ($\omega \sim \omega_{c\alpha}$)	Electromagnetic ion cyclotron wave generation	TF ripple, n_α/n_e	Anomalous loss of both trapped and circulating alphas; ion heating
Alpha population inversion driven Alfvén wave	10^8–10^9 Hz ($\omega \sim 10\,\omega_{c\alpha}$)	$\partial f_\alpha/\partial v > 1$ → alpha cyclotron emission	$\frac{1}{S_\alpha}\frac{\partial}{\partial t}(S_\alpha \tau_\alpha)$	Anomalously slows alphas; emits electromagnetic waves; heats bulk ions

Symbols: $\omega_{d\alpha}$ = alpha precession frequency; ω_A = Alfvén frequency, $\omega_{c\alpha}$ = alpha cyclotron frequency.
$\omega_{*\alpha}$ = alpha diamagnetic frequency.

* This table was prepared with the help of L. Chen, C.Z. Cheng, G. Rewoldt, D. Sigmar and R. White.

effects might be observed have yet to be created. The main purpose of this letter is to show that at least some of this new physics might be tested in present sub-ignited devices.

The basic parameters used to characterize collective alpha effects are n_α/n_e, β_α, V_α/V_A (the alpha speed relative to the Alfvén speed) and, in one case, $P_\alpha(0)/P_{loss}(0)$. The calculations of these parameters are presented in Sections 3–5. Here, we briefly summarize the main physics of these phenomena.

The alpha driven (or modified), very low frequency sawtooth mode is the only one of these instabilities which depends on P_α (through the reheating process). In general, the positive feedback between increased central temperature and increased central heating may cause large sawteeth in the thermonuclear regime [2]. However, if τ_α is longer than typical sawtooth periods, the feedback effect should be relatively weak (as might be the case in TFTR or JET). One interesting physics issue which might be observed on sub-ignited plasmas is the rapid expulsion of alpha particles from inside q = 1 during sawtooth crashes [4]. Stabilization of sawteeth by alphas is also possible at high β_α [5].

Alpha driven fishbones involve a resonance between the precession frequency of trapped alphas and the internal m = 1 mode. White [6] predicted that roughly $\beta_\alpha(0) \approx 1\%$ (with $\beta_{pol}(0) > 0.3$) is necessary for this instability. In analogy to neutral beam injection (NBI) driven fishbones, excitation of large MHD waves and expulsion of banana trapped alphas might be expected; however, the instability frequency for alpha driven fishbones would be approximately ten times higher than for NBI driven fishbones.

Alpha modified drift waves and/or ballooning modes involve the resonance between alphas and pre-existing electrostatic drift or magnetic ballooning modes. Modification of these modes by alphas is potentially important since they are thought to determine tokamak transport and beta limits. The influence of alphas on stability increases with β_α and

the background β_{th}. Existing calculations of such effects for TFTR [7, 8] indicate that alphas decrease the threshold for ballooning instability (i.e. they lower the theoretical beta limit) by >15% but do not significantly affect the drift wave induced transport.

Alpha driven Alfvén waves are the most unfamiliar of these instabilities. Their growth generally requires that energetic particle speeds be greater than the Alfvén speed – a condition that is ordinarily not met by ions created by auxiliary heating but which is met by alphas in TFTR or JET. These instabilities can increase alpha transport, decrease the alpha thermalization time (which may be beneficial if the energy is transferred to background ions) or possibly increase the background plasma transport (through the wave's fields).

Table I shows three different types of destabilization effects for Alfvén waves. A strong enough alpha pressure gradient can excite low-m global Alfvén eigenmodes in plasmas similar to TFTR [9], and both low-m and high-m toroidicity induced Alfvén modes exist when $V_\alpha/V_A > 0.5$ [10]. An alpha loss cone [11] created by toroidal field or MHD induced ripple can potentially create waves which (quasi-linearly) limit the confined alpha population to $n_\alpha/n_e \approx 10^{-4}$. An alpha population inversion [12] caused by a fast turn-on of the alpha source can also create waves which increase the alpha transport.

Alpha heating physics mainly concerns the slow readjustment of the plasma temperature and current profiles to the new alpha heating source function [2]. The classical alpha heating will mainly be central electron heating and so, in some sense, it should be similar to Ohmic heating. Alpha heating will also depend on the confinement of high energy alphas; in this sense, it should be similar to NBI or ICRF heating. The plasma energy confinement time with alpha heating should depend on the plasma instabilities, as usual, including any new alpha instability effects.

These general expectations about alpha heating can be tested to some extent on sub-ignition machines using a strong (but transient) alpha heating pulse, as described below. However, the slow profile changes produced by a dominant alpha heating source can probably not be simulated in sub-ignition machines.

3. ALPHA STORAGE REGIME

An 'alpha storage regime' discharge would consist of three distinct time periods, as shown schematically in Fig. 1. Note that the time-scale in this figure is drawn for a typical TFTR case.

In the 'storing' phase (≈ 2 s) the alphas are created and confined in a high temperature, low density, auxiliary heated D–T plasma similar to a TFTR 'supershot' [1] (but with >1.5 MA for good alpha confinement). By the end of this storing phase, n_α and β_α are maximized, so that any alpha effects on sawteeth, fishbones, ballooning modes or Alfvén waves should be most apparent.

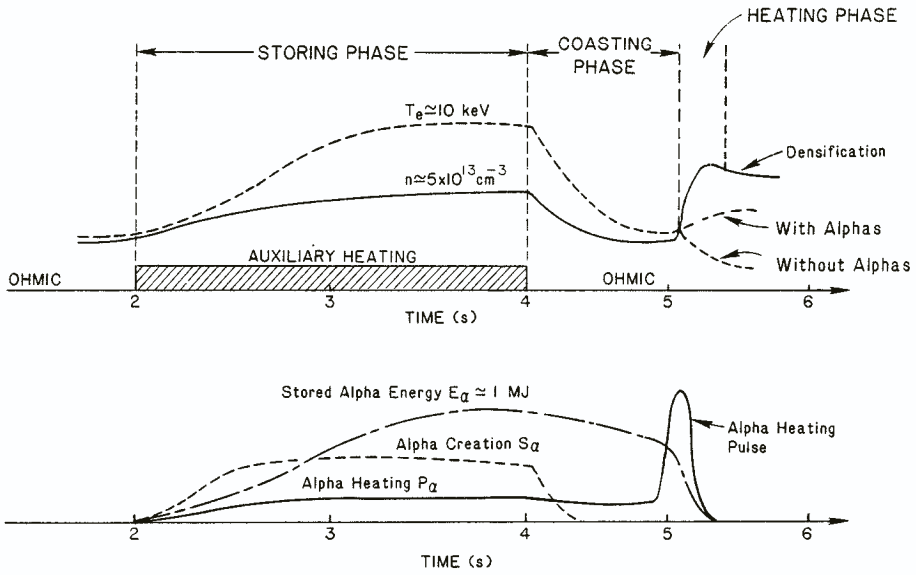

FIG. 1. Schematic time history of an alpha storage regime plasma, with a time-scale appropriate to TFTR.

In the 'coasting' phase (≈ 1 s), just after auxiliary heating ends, the stored alpha energy decreases slowly while the plasma re-establishes a low density Ohmic equilibrium. During this phase, n_α/n_e and β_α/β_{th} are maximized, so that any alpha instabilities persisting at relatively low β_{th} can be studied in the absence of neutral beam ions. In this phase, the stored alpha energy content can also be measured with alpha and possibly with magnetic diagnostics, and compared with the expected classical alpha energy storage.

In the final alpha 'heating' phase (≈ 200 ms) the remaining stored alpha energy is transferred to the background plasma by suddenly decreasing the classical alpha thermalization time. This can be done by increasing the plasma density, as shown (or possibly by decreasing the temperature using impurity injection). In this phase, a dominantly alpha heated plasma is produced, but only for a short time.

In this section the expected alpha parameters for these three phases are estimated using assumed temperatures and densities, while more self-consistent computer simulations for TFTR are presented in Section 4. Note that the simplified estimates given below assume perfect alpha confinement, which may not occur if the plasma current is too low, if the toroidal field ripple is too high, or if instabilities cause anomalous alpha transport.

3.1. n_α/n_e and β_α/β_{th} in the alpha storing phase

Here we use a simple, local steady-state model, applicable to the end of the alpha storing phase, to show that these two alpha instability parameters depend mainly on the plasma temperature and not simply on the fusion power gain Q [13]. The thermonuclear reaction rate for producing alphas is (in the range $T_i \approx 20$ keV):

$$S_\alpha \approx C_1 n_D n_T T_i^{1.5} \tag{1}$$

where $C_1 \approx 1.5 \times 10^{-22}$ m$^3 \cdot$s^{-1} when T_i is in units of 10 keV [14]. The resulting local steady-state alpha populations (assuming perfect alpha confinement) are:

$$n_\alpha = S_\alpha \tau_\alpha \tag{2}$$

where S_α is the local D–T reaction rate, and $\tau_\alpha \approx C_2 T_e/n_e$ is the alpha thermalization time [15], where $C_2 \approx 4.5 \times 10^7$ m$^{-3} \cdot$s at $T_e \approx 10$ keV. Note that this τ_α has a slightly weaker temperature dependence than the $T_e^{3/2}$ dependence of the alpha slowing-down time on electrons [16], since for an alpha energy above $\approx 35\ T_e$ the alphas slow down primarily on ions independently of T_e. Thus,

$$n_\alpha/n_e \approx C_1 C_2 (n_D n_T/n_e^2) T_i^{1.5} T_e \tag{3}$$

When alphas are also produced by non-thermonuclear (beam–target and beam–beam) reactions, there is an additional alpha source rate for any given n and T. This effect can be included simply by defining a new parameter, Ω, to be the total fusion reaction rate divided by the thermonuclear (Maxwellian) fusion reaction rate. Of course, the numerical value of Ω depends upon the shape of the ion distribution function and is difficult to express simply in terms of n and T; however, we know that $1 < \Omega < 4$ is the typical range for neutral beam driven tokamaks [15]. Thus,

$$n_\alpha/n_e \approx C_1 C_2 (n_D n_T/n_e^2) T_i^{1.5} T_e \Omega \tag{4}$$

Thus, for possible TFTR D–T central parameters (see Section 4), $T_i(0) \approx 25$–30 keV, $T_e(0) \approx 10$–12 keV, $n_e(0) \approx (7$–$10) \times 10^{19}$ m^{-3} and $\Omega(0) \approx 2.5$, the central $n_\alpha(0)/n_e(0)$ is comparable to that of an ignited reactor grade plasma at $T_i(0) = T_e(0) = 20$ keV and $\Omega(0) = 1$, assuming that the fuel dilution factor $(n_D n_T/n_e^2)$ is the same for both.

Similarly, the relative alpha beta is

$$\beta_\alpha/\beta_{th} = (2/3) n_\alpha \langle E_\alpha \rangle / [n_e (T_i + T_e)]$$

$$\approx (n_\alpha/n_e)/(T_i + T_e) \tag{5}$$

where the average alpha energy, $\langle E_\alpha \rangle \approx 1.3$ MeV, is only weakly dependent on temperature or density [17]. Thus the relative alpha beta for TFTR is comparable to that of a reactor level ignited plasma, given the parameters above.

These formulas can be used to estimate alpha parameters for the central region of a high temperature TFTR D–T plasma at the end of the alpha storing phase shown in Fig. 1. Near $T_i \approx 20$ keV and $T_e \approx 10$ keV, we obtain from Eq. (4):

$$n_\alpha/n_e \approx 0.7\% (n_D n_T/n_e^2) (T_i/10\ \text{keV})^{1.5} (T_e/10\ \text{keV}) \Omega \tag{6}$$

TABLE II. ALPHA PARTICLE PLASMA PARAMETERS

Parameter	TFTR now*	TFTR objective	'Marginal ignition'[a]	CIT high-T[b]	ITER[c]
Alpha-particle plasma physics					
$n_\alpha(0)/n_e(0)$	0.1–0.2%	1%	0.1%	0.9%	0.7%
$\beta_\alpha(0)$	0.1–0.2%	1%	0.2%	2.5%	2.3%
$V_\alpha/V_{Alfvén}$	1.5–2.0	1.7	2.5	2.6	2.8
Heat flow from a fusion power source					
$P_\alpha(0)/P_{loss}(0)$	0.05–0.1	0.4	~1	~1	~1
$\langle P_\alpha/P_{loss}\rangle$	0.03–0.07	0.2	0.8	~1	~1

* Best results obtained in individual TFTR deuterium plasma supershots (e.g. Nos. 22553, 22984 [1], 26151 and 30969 [23].

[a] $T(0) = 10$ keV, $n(0) = 10^{21}$ m^{-3}, $B = 12.5$ T.
[b] $T(0) = 23$ keV, $n(0) = 6 \times 10^{20}$ m^{-3}, $B = 10$ T.
[c] $T(0) = 20$ keV, $n(0) = 2 \times 10^{20}$ m^{-3}, $B = 5$ T.

Thus, for the possible TFTR central parameters cited above, assuming a possible fuel dilution factor $n_D \approx n_T \approx 0.35\, n_e$ (i.e. $n_D n_T/n_e^2 \approx 0.12$), we find $n_\alpha(0)/n_e(0) \approx 1\%$. Note that for this case the alpha thermalization time is $\tau_\alpha(0) \approx 0.6$ s, so that a typical TFTR alpha storing time of ≈ 2 s is sufficient for the alpha population to reach this steady state value.

Using $\langle E_\alpha\rangle \approx 1.3$ MeV, we obtain from Eq. (5):

$$\beta_\alpha/\beta_{th} \approx (n_\alpha/n_e)\, 90/([T_e + T_i]/10\ \text{keV}) \qquad (7)$$

Thus, for the possible TFTR central parameters cited above, we get $\beta_\alpha(0)/\beta_{th}(0) \approx 0.2$, so at $B = 52$ kG we have $\beta_{th}(0) \approx 5\%$ and $\beta_\alpha(0) \approx 1\%$.

Alternative global scaling forms for these alpha parameters follow directly from the definitions of τ_α and S_α:

$$n_\alpha/n_e \propto P_{heat} Q T_e/(n_e^2 \times \text{plasma volume}) \qquad (8)$$

$$\beta_\alpha \propto P_{heat} Q T_e/(n_e \times \text{plasma volume} \times B^2) \qquad (9)$$

Evaluation of the central alpha parameters for TFTR using these forms requires knowledge of the alpha source radial profile. A typical 'supershot' neutron source profile has $S_\alpha(0)/\langle S_\alpha\rangle \approx 7$–11, corresponding to $S_\alpha(0)/\langle S_\alpha\rangle = (1 - [r/a]^2)^\delta$, where $\delta \approx 6$–10. Thus, with $Q \approx 0.5$, $P_{heat} \approx 30$ MW and central TFTR parameters as above (i.e. $\tau_\alpha(0) \approx 0.6$ s), we get $n_\alpha(0)/n_e(0) \approx \beta_\alpha(0) \approx 1$–1.5%, in rough agreement with the local estimates above.

Table II is a summary of the estimated TFTR alpha parameter 'objectives' for this steady-state alpha storing phase and of the estimated alpha parameters for various proposed ignition devices. TFTR can have $n_\alpha(0)/n_e(0)$ comparable to, and $\beta_\alpha(0)$ close to, these machines.

3.2. Coasting phase

After auxiliary heating is turned off, the stored alpha population decays over a thermalization time of $\approx \tau_\alpha$ in a plasma which returns to a low density Ohmic equilibrium over $\approx 2\tau_E$ ($\approx 2\tau_p$), mainly through a decrease in density, as shown schematically in Fig. 1. If $\tau_\alpha \gg \tau_E$ during this phase, then the alpha parameters n_α/n_e and β_α/β_{th} will increase (compared to the end of the storing phase) owing to these decreases in n_e and β_{th}, typically by factors of two to three. Time dependent simulations of the coasting phase for TFTR are described in Section 4.3.

3.3. Alpha heating phase

Alpha heating at the end of the storing phase is limited globally to $\langle P_\alpha/P_{heat}\rangle \approx 0.2$ Q, i.e. typically 20% for Q ≈ 1. Such heating should be a measurable but not a dominant effect in TFTR or JET. This alpha heating is normally concentrated in the centre of the plasma [18], where

$$P_\alpha(0) = S_\alpha(0)E_\alpha = C_1\, n_D(0)\, n_T(0)\, T_i^{1.5}(0)\, E_\alpha \Omega(0) \tag{10}$$

$$P_{loss} = \{1.5[(n_D(0) + n_T(0) + n_c(0))\, T_i(0) + n_e(0)T_e(0)]\}/\tau_E(0)$$

where $E_\alpha = 3.5$ MeV and $n_c(0)$ is the central impurity (carbon) density. Typically, $P_\alpha(0)/P_{loss}(0) \approx 0.3$–$0.4$ for Q ≈ 1 plasmas (see Section 4.2). This level of central alpha heating is probably measurable, but again not at the reactor relevant level $P_\alpha(0)/P_{heat}(0) \approx P_\alpha(0)/P_{loss}(0) \approx 1$.

One way to further increase alpha heating at Q ≈ 1 is to concentrate it in *time* by using previously stored alpha energy to supply a transient alpha heating pulse after auxiliary heating is turned off, as shown schematically in Fig. 1. Here we estimate the maximum available $P_\alpha(0)/P_{heat}(0)$ and $\langle P_\alpha/P_{heat}\rangle$ for such a heating pulse.

To obtain a large alpha heating pulse in the way indicated schematically in Fig. 1, several time-scales must be considered. First, the beam heating power should decay before the alpha heating phase begins. This happens automatically since the thermalization time for ≈100 keV deuterium beam ions is $\tau_b \approx 0.3\,\tau_\alpha$ [4]. Next, the alpha thermalization time just after beam injection should be longer than the plasma energy confinement time after beam injection, in order to allow the plasma to re-establish an Ohmic equilibrium before the alpha heating begins (to simplify the alpha heating analysis). This is possible if the density is allowed to decay rapidly after beam turn-off, since $\tau_\alpha > 1$ s while $\tau_E \approx 200$–300 ms in low density Ohmic TFTR discharges [18]. Finally, the time-scale for alpha thermalization after re-densification, τ_α^*, should be as small as possible to obtain the maximum alpha heating effect, but large enough to avoid complicated profile changes, i.e. $\tau_\alpha^* \approx 100$–$300$ ms. This time-scale determines the required density rise.

Assuming that all these time-scales are optimized, we can estimate the local and global alpha heating parameters in this scenario. For the local central TFTR parameters used above, we had $n_\alpha(0) \approx 10^{18}$ m^{-3} and $\langle E_\alpha\rangle \approx 1.3$ MeV. Thus, if *half* (see Section 4.4) of the stored alpha energy is retained until it is re-thermalized over $\tau_\alpha^* \approx 200$ ms during the alpha heating phase, we have

$$P_\alpha(0) \approx n_\alpha(0)\langle E_\alpha\rangle/\tau_\alpha^* \approx 10^6\ \text{W}\cdot\text{m}^{-3} \tag{11}$$

locally. Since the central Ohmic heating power in TFTR for $q(0) \approx 1$ and I ≈ 2 MA is $P_{heat} \approx 0.2 \times 10^6$ W·m^{-3}, we have roughly

$$P_\alpha(0)/P_{heat}(0) \approx 0.8 \tag{12}$$

at the centre during this transient alpha heating phase, i.e. alpha heating would be dominant locally.

The global alpha heating can be related to the total stored alpha energy just before re-densification, W_α^*, which in turn is related to the total stored alpha energy W_α at the end of the alpha storing phase. W_α can be related to Q through an average alpha thermalization time

$$W_\alpha \approx 0.2Q\, P_{heat}\, \langle\tau_\alpha\rangle\, [\langle E_\alpha\rangle/3.5\ \text{MeV}] \tag{13}$$

For TFTR, Q ≈ 1, $P_{heat} \approx 30$ MW, $\langle\tau_\alpha\rangle \approx 0.5$ s and $\langle E_\alpha\rangle \approx 1.3$ MeV, so we have $W_\alpha \approx 1$ MJ. If half of this energy remains to be thermalized by re-densification over $\tau_\alpha^* \approx 200$ ms (as assumed above), we obtain $\langle P_\alpha\rangle \approx 2.5$ MW, while $\langle P_{Ohmic}\rangle \approx 2$ MW, so that

$$\langle P_\alpha/P_{heat}\rangle \approx 0.5 \tag{14}$$

Therefore, global alpha heating would be larger than in the beam heated alpha storing phase.

The effect of this alpha heating should be to raise the stored energy of the thermal background plasma, W_{th}, at the expense of the stored alpha energy. Since, for a typical low density ohmically heated plasma, $W_{th} < 0.5$ MJ [19], the increase due to the above value of W_α^* should ideally more than double the thermal stored energy.

The following section presents more detailed simulations of these scenarios for TFTR.

4. ALPHA STORAGE SIMULATION RESULTS FOR TFTR

Two different plasma simulation codes were used to calculate the alpha particle parameters expected for full-power TFTR D–T plasmas. Section 4.1 presents the results from a relatively simple time-independent code, SURVEY, which was used to calculate alpha parameters for the steady state 'storing' phase of a wide range of TFTR plasmas. Sections 4.2–4.4 give results from a time-dependent code, BALDUR, which created detailed simulations for all three phases for a few TFTR scenarios. In general, the results of these two codes are consistent with each other and with the simplified estimates given in Section 3.

4.1. SURVEY simulation results

The time-independent code SURVEY was developed to survey the parameter space $\bar{n}_e$ versus τ_E to find regimes of $Q \approx 1$. The code assumes density and temperature profile shapes and calculates the temperatures, Q-values and other parameters versus $\bar{n}_e$ from an assumed τ_E and input power. Several realistic features are taken into account, such as the input power profile, the fuel density dilution due to beam and impurity ions, beam–target and beam–beam reactions, electron–ion coupling and alpha particle heating.

Typical alpha particle results from this code versus $\bar{n}_e$ are shown in Figs 2 and 3. In these examples, the input plasma density and temperature profile shapes were taken from a TFTR supershot which had a density profile peaking factor $n_e(0)/\bar{n}_e = 2.3$, while the input power was 27 MW of NBI (50% in D and 50% in T), and an optimistic $Z = 1.5$ (from carbon) was assumed.

The basic result as shown in Fig. 2 was that for a fixed τ_E the central alpha instability parameters increased rapidly with decreasing $\bar{n}_e$, reaching $n_\alpha(0)/n_e(0) \approx \beta_\alpha(0) \approx 1\%$ at $\bar{n}_e \approx 4.5 \times 10^{19}\ m^{-3}$ (i.e. $n_e(0) \approx 10^{20}\ m^{-3}$) for $\tau_E \approx 0.2$ s and $Q \approx 0.75$. This trend is mainly due to the increasing temperature at low density implicit in the assumption that τ_E is independent of density, which causes the alpha thermalization time, $\tau_\alpha \propto T_e/n_e$, to increase rapidly at low $\bar{n}_e$. The increased alpha population at low density is also caused in part by the increased Ω due to beam–target and beam–beam reactions (see Eq. (4)). For example, Ω varies between 1.6 and 4.4 as $\bar{n}$ is varied between $1.2 \times 10^{20}\ m^{-3}$ and $4.5 \times 10^{19}\ m^{-3}$ along the $Q = 0.5$ curves in Fig. 2.

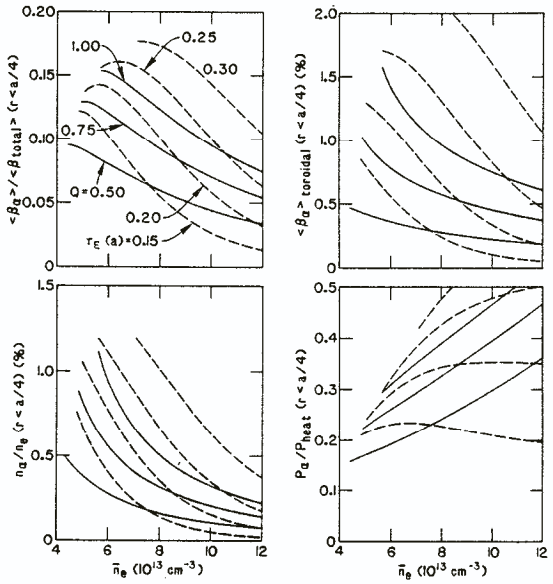

FIG. 2. SURVEY code results for steady state alpha parameters in TFTR. The four graphs are for central (i.e. $r < a/4$) β_α/β_{tot}, β_α, n_α/n_e and P_α/P_{heat}. For each graph, lines of constant τ_E (dashed) and Q (solid) are shown.

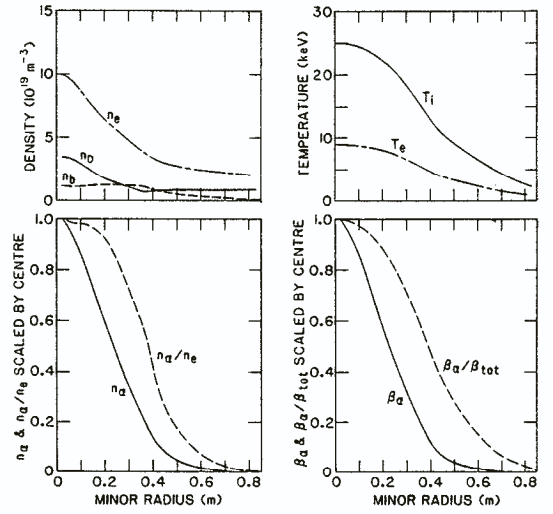

FIG. 3. SURVEY code results for radial profiles of alpha parameters for TFTR. The density and temperature profiles are fixed to be similar to TFTR supershots. The resulting alpha parameters are strongly centrally peaked, as expected. The central values for this case are $n_\alpha(0) = 5.2 \times 10^{17}\ m^{-3}$, $n_\alpha(0)/n_e(0) = 0.52\%$, $\beta_\alpha = 0.65\%$ and $\beta_\alpha(0)/\beta_{tot}(0) = 10\%$. Note that only the deuterium ion and beam density curves are shown; the tritium ion and beam densities are equal to those for deuterium.

TABLE III. SIMULATIONS OF THE ALPHA STORAGE REGIME IN D-T TOKAMAKS

	TFTR results[a]	Simulated storing phase (A)	(B)	Simulated coasting phase (C)	(D)
Time (s)	4.5	4.7	4.7	5.3	5.3
Q	0.25	0.47	0.38	–	–
P_{NB} (MW)	15	30	30	–	–
P_{RF} (MW)	0	0	7.5	–	–
n_e (10^{19} m^{-3})	2.3	3.4	3.0	1.3	1.2
$n_e(0)$ (10^{19} m^{-3})	6.5	6.7	5.6	2.1	2.0
$T_e(0)$ (keV)	7.5	12.0	16.4	13	15.2
$T_i(0)$ (keV)	22	28.0	44.0	13	16.5
Z_{eff}	3	1.3	1.3	1.3	1.3
τ_E (s)	0.17	0.19	0.19	0.28	0.21
B (T)	5.2	5.0	5.0	5.0	5.0
I_p (MA)	1.0	3.0	3.0	3.0	3.0
β_{Troyon} (%)	0.7	2.2	2.2	2.2	2.2
$\langle\beta\rangle$ (%)	0.5	1.3	1.5	0.32	0.41
$\beta_{th}(0)$ (%)	2.0	3.3	4.2	0.8	0.9
$\tau_\alpha(0)$ (s)	0.5	0.76	1.2	2.5	3.1
$\langle\beta_\alpha\rangle$ (%)	0.02	0.13	0.19	0.09	0.15
$\beta_\alpha(0)$ (%)	0.15	1.0	1.4	0.65	1.0
$n_\alpha(0)/n_e(0)$ (%)	0.15	1.0	1.7	2.4	4.0
W_α (MJ)	0.15	0.92	1.3	0.64	1.0
$\langle P_\alpha/P_{heat}\rangle$	0.05	0.10	0.08	0.48	0.51
$P_\alpha(a/4)/P_{heat}(a/4)$	0.07	0.11	0.05	0.66	0.67
$\langle P_\alpha/P_{loss}\rangle$	0.05	0.10	0.08	0.11	0.10
$P_\alpha(a/4)/P_{loss}(a/4)$	0.07	0.11	0.05	0.17	0.18
Ω	4	2.5	2.3	–	–

[a] Present plasma parameters from Ref. [1] ('storing' phase).

Also shown in Fig. 2 is the central $P_\alpha(0)/P_{heat}(0)$ versus $\bar{n}_e$, which peaks at higher density than the other two alpha parameters. This variation is mainly due to decreased central NBI heating power at higher density and not to increased central alpha heating power. A central $P_\alpha(0)/P_{heat}(0) \approx 0.3$–$0.4$ can be obtained in steady state because of the spatial concentration of alpha heating.

Figure 3 shows the radial profiles of alpha parameters and other relevant quantities for a case at the low density limit, with $Q \approx 0.5$, $\tau_E \approx 0.10$ s and $\bar{n}_e \approx 4.5 \times 10^{19}$ m^{-3}. The alpha density and beta are strongly centrally peaked, as expected, with $\delta \approx 7$ (in the notation of Section 3.1).

The general conclusion from this code is that operation at the lowest possible density maximizes the alpha instability parameters n_α/n_e and β_α, given the usual trend that τ_E is independent of density in strongly heated plasmas [19].

4.2. BALDUR results for the alpha storing phase

The 1-D time-dependent code BALDUR [20] was used to simulate several different alpha storage scenarios in more detail than was possible with the SURVEY code. BALDUR calculates the density and temperature profiles self-consistently, given the auxiliary heating power, the recycling coefficient, assumed

forms for the electron and ion heat and particle transport coefficients, etc. BALDUR also includes a finite banana width classical alpha confinement (without ripple losses) and a classical slowing-down model in calculating alpha particle densities and heating.

Typical results for the steady state alpha storing phase at the end of a 2 s long auxiliary heating pulse are shown in columns (A) and (B) of Table III. Of course, since these transport coefficients and Z_{eff} are not yet known for anticipated $Q \approx 1$ conditions, these simulations should be considered as idealized rather than realistic predictions of TFTR D–T performance.

Column (A) of Table III shows results for a nearly optimal TFTR D–T alpha 'storing' plasma with high power (30 MW of NBI), low density ($n_e(0) \approx 7 \times 10^{19}$ m^{-3}), relatively good confinement time ($\tau_E \approx 0.19$ s), moderate Q (0.47), high current (3 MA) and low Z_{eff} (1.3). This simulation resulted in the following central alpha parameters: $n_\alpha(0)/n_e(0) = 1\%$, $\beta_\alpha \approx 1\%$, $\beta_\alpha(0)/\beta_{th}(0) = 0.3$ and $P_\alpha(0)/P_{loss}(0) \approx 0.1$.

These results can be compared with the simplified estimates given in Section 3. Application of Eqs (6) and (7), using BALDUR's central parameters, gives $n_\alpha(0)/n_e(0) = 1\%$ and $\beta_\alpha(0)/\beta_{th}(0) = 0.25$, which agrees with BALDUR's estimates to well within a factor of two. The central alpha heating parameter $P_\alpha(0)/P_{loss}(0)$ as calculated through the simplified estimate of Eq. (8) also agrees to within a factor of two with BALDUR's estimate of $P_\alpha(0)/P_{loss}(0) \approx 0.1$. The global alpha heating was $\langle P_\alpha/P_{loss}\rangle \approx 0.1$, as expected for $Q \approx 0.5$.

Column (B) of Table III gives the results of an identical BALDUR run, except for an added 7.5 MW of central ICRF heating. The central temperatures increase by about 40% and the central $n_\alpha(0)/n_e(0)$ and $\beta_\alpha(0)$ values increase by about 50%. This example shows that central plasma heating is very effective in increasing the central alpha parameters if, as assumed here, the plasma confinement does not degrade substantially with added power. Note also that in this simulation it was assumed that ICRF heating does not introduce additional fuelling, which is not always the case experimentally because of ICRF induced impurity influx.

The predicted $n_\alpha(0)/n_e(0)$ and $\beta_\alpha(0)$ values from these BALDUR simulations are also roughly consistent with the SURVEY code results for the same assumed heating power, confinement time, impurity level and plasma density (and with a previous low density BALDUR simulation [3]). Of course, both these results depend on the degree to which the assumptions in these codes match the reality of such discharges, which have yet to be produced. A comparison with the present experimental results is presented in Table III and discussed in Section 5.

4.3. BALDUR results for the coasting phase

Columns (C) and (D) of Table III give results of the same simulations as used for columns (A) and (B), respectively, but for a time 500 ms after the end of the NBI heating phase, at which time the beam ion density is negligible. It is interesting to note that the central alpha instability parameters $n_\alpha(0)/n_e(0)$ and $\beta_\alpha(0)/\beta_{th}(0)$ actually increase by a factor of two to three after beam turn-off, as anticipated in Section 3.2, mainly because of the rapid decrease of $n_e(0)$ to its pre-NBI level of $\approx 2 \times 10^{19}$ m^{-3} at the end of beam fuelling. This coasting phase can be used to look for alpha instabilities and to check the classical modelling of alpha confinement and thermalization without the (possibly) competing effect of NBI-driven instabilities. The alpha beta during this phase may be directly measurable through the difference between the magnetic (total) and kinetic (thermal) betas.

Also interesting is the relatively high central and global alpha heating, $\langle P_\alpha/P_{heat}\rangle \approx P_\alpha(0)/P_{heat}(0) \approx 0.5$, after beam turn-off, due mainly to the rapid decay of beam heating. However, even though the alpha heating in these cases is relatively strong compared to other heating sources, the decay of thermal energy after NBI still dominates the power balance at this time, such that $\langle P_\alpha/P_{loss}\rangle \approx P_\alpha(0)/P_{loss}(0) \approx 0.1$ at 500 ms after NBI. Thus the net thermal stored energy during this phase is still decreasing despite the alpha heating (since $P_{loss} > P_{heat}$ until Ohmic equilibrium is completely re-established).

4.4. BALDUR results for the alpha heating phase

Figure 4 presents the results of a BALDUR run similar to that used to obtain the values given in column (B) (and column (D)) of Table III, but with a pellet injected 0.9 s after beam turn-off to thermalize the stored alpha energy, as shown schematically in Fig. 1. Pellet injection was timed to be late enough so that the plasma had nearly re-established an Ohmic equilibrium, but early enough so that a significant fraction of the original stored alpha energy ($\approx$50%) remained in the plasma. This run used a relatively small pellet, which increased $\bar{n}_e$ from 1.2×10^{19} m^{-3} to 2.2×10^{19} m^{-3} (and increased the volume averaged density $\langle n_e\rangle$ by about a factor of two).

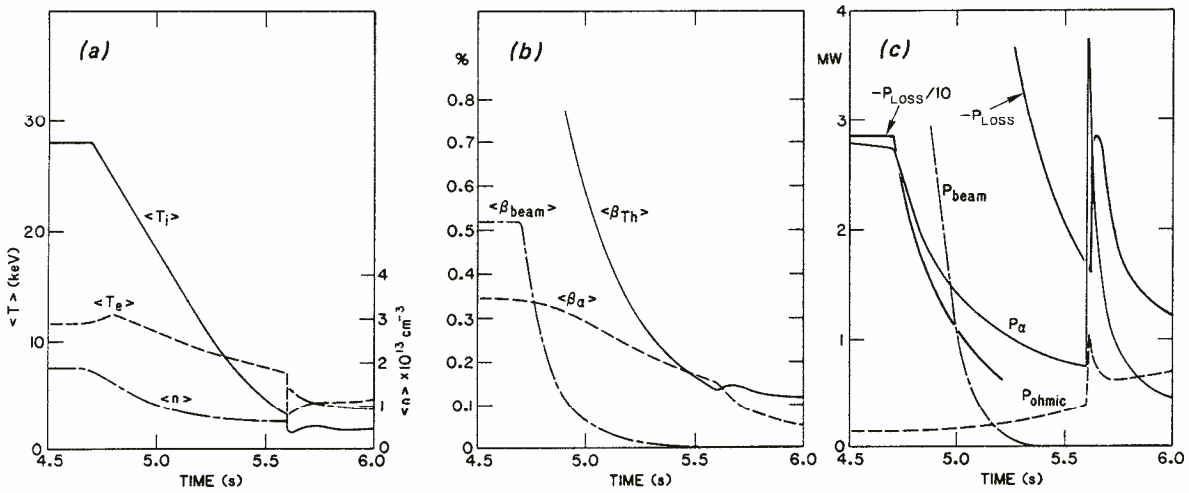

FIG. 4. BALDUR code results for the alpha coasting and alpha heating phases of a $Q \approx 0.5$ TFTR case: (a) Volume averaged temperatures and densities; (b) volume averaged betas for alphas, beams and the thermal plasma; (c) total powers for alpha, beam and Ohmic heating and the total power loss rate.

Starting with the pellet densification at 5.6 s, about 50% of the stored alpha energy was thermalized in ≈200 ms, as shown by the drop in $\langle\beta_\alpha\rangle$ in Fig. 4. Thus the average alpha heating over this time $\langle P_\alpha\rangle$ was ≈1.5 MW, while the average Ohmic heating $\langle P_{Oh}\rangle$ was ≈0.7 MW. As a result of this heating, the average thermal stored energy $\langle\beta_{th}\rangle$ increased by about 25% above the value it would have had with pellet injection but without alpha heating. The increase in global thermal energy content due to alpha heating could be measured by the standard thermal plasma kinetic and/or magnetic diagnostics.

Another run was made with a larger pellet; in this run, $\langle n_e\rangle$ was increased by a factor of five instead of a factor of two, in an attempt to increase the alpha heating pulse. In that case, the average alpha heating over 200 ms was increased from ≈1.5 MW (previous run) to ≈3 MW, and the increase in thermal stored energy at 5.8 s was about 50% instead of 25%. On the other hand, the large changes in $\langle T\rangle$ and $\langle n_e\rangle$ and their profiles that would be induced by the pellet would make an interpretation of alpha heating effects difficult. Perhaps the use of a more gentle neutral gas 'puff' rather than a pellet would be more appropriate.

5. PRESENT TFTR CAPABILITIES

In this section we consider the alpha particle parameters which would be obtained if the existing TFTR plasmas were run with D–T fuel. The fuelling is assumed to be from a 50%/50% mixture of nominal 120 keV deuterium and tritium neutral beams.

The present TFTR central alpha parameters can be estimated by using the simplified analysis of Section 3. For the original 'supershot' central plasma parameters [1], as summarized in Table III, we find, using Eqs (6) and (7) (with $n_D(0)n_T(0)/n_e(0)^2) = 0.062$ and $\Omega(0)=4$, that $n_\alpha(0)/n_e(0) \approx 0.3\%$ and $\beta_\alpha(0) \approx 0.3\%$, both with about ±50% uncertainty. The same result can be obtained by using the global forms in Eqs (8) and (9) with $\tau_\alpha(0) \approx 0.5$ s, $P_{heat} = 15$ MW, $Q_{eq} \approx 0.25$ and $S_\alpha(0)/\langle S_\alpha\rangle \approx 9$ (consistent with the calculated neutron source profile for this shot).

An independent estimate was made, using a SURVEY code model of a more recent TFTR supershot, with $T_i(0) = 26.2$ keV, $T_e(0) = 7.8$ keV, $n_e(0) = 6 \times 10^{19}$ m^{-3}, $n_D n_T/n_e^2 = 0.085$, B = 52 kG, I = 0.9 MA, Q = 0.22, $P_{heat} = 13$ MW and $\tau_E = 0.11$ s. The results were: $n_\alpha(0)/n_e(0) \approx 0.28\%$ and $\beta_\alpha(0) \approx 0.17\%$, which is roughly consistent with the other two estimates.

Global alpha heating levels for present TFTR plasmas in the steady state near the end of the storing phase would be $\langle P_\alpha/P_{Loss}\rangle \approx 0.05$, since $Q \approx 0.25$. At present, the central alpha heating according to the estimate of Eq. (10) is $P_\alpha(0)/P_{Loss}(0) \approx 0.1$ (with $P_\alpha(0) \approx 0.2 \times 10^6$ W·m^{-3} and $P_{loss}(0) \approx 2 \times 10^6$ W·m^{-3}), which is roughly consistent with the SURVEY run for a similar plasma, as mentioned above.

The preceding estimates for present TFTR results must be corrected for the imperfect neoclassical alpha confinement for the original 'supershot' plasma currents of only ≈1 MA. The prompt-loss fraction for alphas inside r/a = 0.3 is ≈25% (from a 1 MA BALDUR run), and the finite banana width of centrally born alphas further reduces the central alpha density by ≈20%. Thus the above estimates should be divided by ≈2 to give the present TFTR central alpha parameter range, i.e. $n_\alpha(0)/n_e(0) \approx \beta_\alpha(0) \approx 0.1$–$0.2\%$ and $P_\alpha(0)/P_{loss}(0) \approx 0.05$–$0.1$ (recently, 1.4–1.6 MA supershots have been achieved for which this correction would be almost negligible).

It should also be noted that any additional 'single-particle' alpha losses, such as those due to toroidal field ripple or interactions with MHD instabilities, will further reduce these alpha parameters. Of course, the main objective of these experiments is to determine whether any additional 'collective' alpha losses also exist.

For the coasting phase, the main concern is the density and temperature evolution after auxiliary heating. For the 1 MA 'supershot' referred to above [1], the existing plasmas are roughly similar to the simulations with respect to the expected two- to threefold increases in n_α/n_e and β_α/β_{th} in the coasting phase relative to the storing phase.

Recent TFTR experiments on the burnup of 1 MeV tritons have analysed this coasting phase in some detail [21]. It was shown that these tritons, which are created in D–D reactions during the storing phase and which should have slowing-down times and confinement properties similar to alphas, were confined for ≈1 s during the coasting phase. This is very long, as expected, but still somewhat less than the simulation result of $\tau_\alpha \approx 2$–3 s for this phase (Table III) because of the lower T_e in the present experiments.

Densification of TFTR plasmas during the coasting phase has also been tried recently by injecting 3.5 mm diameter deuterium pellets into the low density plasmas 0.25–1.5 s after NBI [22]. For pellet injection at 0.75 s after NBI, $\bar{n}_e$ increased tenfold and n(0) increased sevenfold, i.e. far more than is necessary to realize the simulation of Fig. 4. In this case, the alpha thermalization time was reduced to $\tau_\alpha \approx 10$ ms near the centre, and a corresponding transient increase in the triton burnup similar to transient alpha heating was observed. However, the density and temperature profiles were very distorted and a large sawtooth-like event was observed just after pellet injection. Thus, for practical purposes, either a much smaller pellet (which would not penetrate to the centre) or gas puffing should be used for densification.

6. CONCLUSIONS

We have described a high temperature 'alpha storage regime' in which reactor relevant alpha instability parameters, n_α/n_e and β_α, can be obtained even in the present generation of sub-ignited D–T tokamaks such as TFTR or JET. These plasmas can be used to test theoretical models of potential alpha instabilities, such as alpha fishbones, alpha-modified ballooning modes and/or alpha-driven Alfvén waves.

The experimental scenario used to exploit this regime in TFTR consists of an alpha 'storing' phase during auxiliary heating, an alpha 'coasting' phase in which the alphas remain after the beam heating ends, and an alpha 'heating' phase during which the remaining alpha energy is collisionally transferred to the background plasma. Simple estimates and computer simulations were used to find the expected alpha parameters for present and anticipated TFTR conditions.

A comparison between the alpha parameters for TFTR and those expected for various ignition machines is given in Table II. The relative alpha densities in TFTR could be comparable to or higher than those in ignited plasmas. The alpha betas in TFTR could be higher than those in low temperature ignition devices, and within about a factor of 2.5 of those in high temperature ignition devices (which run at higher thermal beta than TFTR). The parameter $V_\alpha/V_{Alfvén}$ is lower in TFTR than in higher density ignition devices, but it is still high enough to potentially excite Alfvén wave instabilities. The alpha power source in TFTR is, of course, less dominant than in ignition devices, but its heating effects should be measurable both in steady-state and transient experiments.

It can be concluded that TFTR or JET can explore reactor-relevant alpha instability and confinement physics, and can be useful for a preliminary study of alpha heating physics.

ACKNOWLEDGEMENTS

The authors thank G. Bateman, L. Chen, C.Z. Cheng, R. Goldston, D. Jassby, D. Meade, D. Post, G. Rewoldt, P. Rutherford, G. Schmidt, D. Sigmar and R. White for many helpful comments.

This work was supported by the United States Department of Energy, under Contract No. DE-AC02-76-CHO3073.

REFERENCES

[1] STRACHAN, J.D., BITTER, M., RAMSEY, A.T., et al., Phys. Rev. Lett. **58** (1987) 1004.

[2] SIGMAR, D.J., Phys. Scr. **16** (1987) 6.
SIGMAR, D.J., Summary of the Discussion Meeting on Alpha Particle Theory Problems, Rep. PFC/CP-88-1, Plasma Fusion Center, Massachusetts Institute of Technology, Cambridge (1988).

[3] ZWEBEN, S., Phys. Scr. **16** (1987) 119.

[4] MARTIN, G., JARVIS, O.N., KÄLLNE, J., et al., Phys. Scr. **167** (1987) 160.

[5] WHITE, R.B., RUTHERFORD, P.H., COLESTOCK, P., BUSSAC, M.N., Phys. Rev. Lett. **60** (1988) 2038.

[6] WHITE, R., in Alpha Particle Effects (Proc. Workshop New York, 1985), Courant Institute of Mathematical Sciences, New York University, New York (1985).

[7] REWOLDT, G., Alpha Particle Effects on High-n Instabilities in Tokamaks, Rep. PPPL-2532, Princeton Plasma Physics Laboratory (1988), to be published in Phys. Fluids, Dec. 1988.

[8] SPONG, D.A., SIGMAR, D.J., RAMOS, J.J., Fusion Technol. **13** (1988) 428.

[9] LI, Y.M., MAHAJAN, S.M., ROSS, D., Phys. Fluids **30** (1987) 1466.

[10] CHENG, C.Z., CHANCE, M.S., Phys. Fluids **29** (1986) 3695;
CHENG, C.Z., CHEN, L., CHANCE, M.S., Ann. Phys. (N.Y.) **161** (1984) 21.

[11] ANDERSON, D., LISAK, M., Phys. Fluids **27** (1984) 925.

[12] SIGMAR, D.J., in Physics of Plasmas Close to Thermonuclear Conditions (Proc. Course Varenna, 1979), Vol. 1, EUR-FU-BRU/XII/476/80, CEC, Brussels (1979) 271.

[13] HOULBERG, W., in Alpha Particle Effects (Proc. Workshop New York, 1985), Courant Institute of Mathematical Sciences, New York University, New York (1985).

[14] SADLER, G., VAN BELLE, P., An Improved Formulation of the D(t,n)^{4}He Reaction Cross-section, Rep. JET-IR (87) 08, JET Joint Undertaking, Abingdon, Oxfordshire (1987).

[15] JASSBY, D., Nucl. Fusion **17** (1977) 309.

[16] POST, D., in Applied Atomic Collision Physics, Vol. 2, Academic Press, New York (1984) 381.

[17] JASSBY, D., Nucl. Fusion **15** (1975) 453.

[18] REDI, M.H., ZWEBEN, S.J., BATEMAN, G., Fusion Technol. **13** (1988) 57.

[19] HAWRYLUK, R.J., ARUNASALAM, V., BELL, M.G., in Plasma Physics and Controlled Nuclear Fusion Research 1986 (Proc. 11th Int. Conf. Kyoto, 1986), Vol. 1, IAEA, Vienna (1987) 51.

[20] SINGER, C.E., POST, D.E., MIKKELSEN, D.R., et al., Comput. Phys. Commun. **49** (1988) 275;
REDI, M.H., Comput. Phys. Commun. **49** (1988) 399.

[21] BARNES, C.W., BOSCH, H.-S., NIESCHMIDT, E.B., et al., in Controlled Fusion and Plasma Heating (Proc. 15th Eur. Conf. Dubrovnik, 1988), Vol. 12B, Part I, European Physical Society (1988) 87.

[22] MURPHY, T., BARNES, C.W., SCHMIDT, G., et al., ibid., p. 91.

[23] ZARNSTORFF, M., BELL, M.G., BITTER, M., et al., ibid., p. 95.

(Manuscript received 24 June 1988
Final manuscript received 7 September 1988)

ICRF WAVE ABSORPTION BY ALPHA PARTICLES

M. YAMAGIWA, T. TAKIZUKA (Department of Thermonuclear Fusion Research, Japan Atomic Energy Research Institute, Naka, Ibaraki, Japan)

ABSTRACT. Absorption of ICRF waves by alpha particles is investigated. Higher harmonic cyclotron damping of the waves is examined not only for the slowing-down distribution of alpha particles but also for the distribution given by the Fokker–Planck calculation. The right and left hand circularly polarized amplitudes of the RF electric field are taken into account in the RF diffusion coefficient. The linear absorption rate for the alpha slowing-down distribution increases with decreasing ratio of electron plasma to electron cyclotron frequency and increasing cyclotron harmonic number. Unless this absorption rate is nearly unity, the bulk formation of alpha particles results in a further increase of the rate of absorption by alphas. Fusion reactivity enhancement due to the ICRF induced ion tail and fusion energy multiplication in the presence of alpha particles are also discussed.

Radiofrequency (RF) waves are considered useful for current drive and plasma heating in tokamak plasmas. Alpha particles in a reactor plasma can affect propagation and absorption of the RF waves. Wong and Ono showed that energetic alpha particles tend to absorb both slow and fast waves in the lower hybrid frequency range, which may be a serious obstacle to tokamak reactor current drive [1]. According to Bonoli and Porkolab [2], however, significant alpha particle damping of the slow wave may be avoided because wave propagation is restricted to the outer plasma region by the conditions for wave accessibility and electron Landau damping and the alpha particle density profile is peaked near the plasma centre. The same drawback of wave absorption by alpha particles may be expected from current drive by fast waves in the ion cyclotron range of frequencies (ICRF). Provided that the ICRF waves used to heat the plasma up to ignition temperature are wasted by the alpha particles produced, the heating efficiency of the fuel ions could